COMPDYN 2015
5th ECCOMAS Thematic Conference on
Computational Methods in Structural Dynamics and Earthquake Engineering
M. Papadrakakis, V. Papadopoulos, V. Plevris (eds.)
Crete Island, Greece, 25–27 May 2015

NUMERICAL SEISMIC SAFETY ASSESSMENT OF RC BRIDGES WITH HOLLOW PIERS

Pedro Delgado[1], António Arêde[2], Nelson Vila Pouca[2], and Aníbal Costa[3]

[1] Instituto Politécnico de Viana do Castelo
Apartado 574, 4901-908 Viana do Castelo, Portugal
pdelgado@estg.ipvc.pt

[2] Universidade do Porto - Faculdade de Engenharia
R. Dr. Roberto Frias, s/n 4200-465 Porto, Portugal
aarede@fe.up.pt, nelsonvp@fe.up.pt

[3] Universidade de Aveiro
Campus Universitário de Santiago, 3810-193 Aveiro, Portugal
acosta@civil.ua.pt

Keywords: RC Bridges; Structural Modeling; Safety Assessment; Non-linear behavior.

Abstract. *The seismic damages of reinforced concrete bridges in recent events show that many of them have an inadequate behavior and safety. Therefore, is important to accurately define bridge safety assessment and hence evaluate the accuracy of the analytical methodologies for seismic response of bridges. The main objective of this paper is to present several options for structural simulation with different complexities in order to assess the seismic response of bridges and then use the results for the safety assessment with probabilistic approaches. The numerical simulations are carried out using three different methodologies: (i) plastic hinge model, (ii) fiber model and (iii) damage model. Seismic response of bridges is based on a simplified plane model, with easy practical application and involving reduced calculation efforts while maintaining adequate accuracy. The evaluation of seismic vulnerability is carried out through the failure probability quantification involving a non-linear transformation of the seismic action in its structural effects. The applicability of the proposed methodologies is then illustrated in the seismic analysis of two reinforced concrete bridges, involving a series of experimental tests and numerical analysis, providing an excellent set of results for comparison and global calibration.*

1 INTRODUCTION

In the evaluation of the seismic vulnerability of bridges, considering their non-linear behavior (a necessary consideration when a realistic analysis of the seismic response is intended) could involve enormous computing resources and corresponding calculation efforts. On the other hand, the development of research studies in this field has enabled a better understanding of their behavior, and the availability of numerical and experimental results allows the possibility of the calibration of simplified procedures.

However very high refined models could be adopted, involving a 3D space modelling and the spread of the plasticity along the member length as well as across the section area, in this work a substantial more simplified model (without losing accuracy) is also explored. This simplicity is evidenced by a much lower number of parameters involved and an enormous lesser computing time – about 50 times less when compared with a more refined model. Therefore, the adoption of such simplified model shows the great advantage, from the practical use point of view, when a large number of analysis is needed, as is the case of vulnerability analysis.

Several examples of numerical modeling can be mentioned, in particular, the fiber model [1-3], the continuous damage model developed by Faria *et al.* [4], the model of compression field theory modified [5], plastic hinge type models Takeda [6] and models based on distributed flexibility [7]. Some other numerical studies focusing on pier finite element modelling can also be found in the literature [8-10], which addressed the simulation of 3D pier behavior by considering several models ranging from elasto-plastic to microplane formulations for solid section piers. An approach based on a fracture-plastic model was also proposed and used for 3D numerical modelling of hollow piers in a more recent work [11,12], which discusses issues related with concrete confinement.

2 METHODOLOGIES FOR NON-LINEAR ANALYSIS

For the numerical simulations of bridge elements three main different methodologies were used. The plastic hinge model have adopted a simplified structural modelling with 2D characteristics and the non-linear behavior lumped in the elements extremities (plastic hinges). The fiber model considered a finite element mesh with non-linear behavior spread along the elements and cross sections. The more complex and detailed numerical model used in this work is the damage model, which is based on refined finite element meshes and the non-linear behavior considered in the constitutive laws defined for both concrete and steel materials.

2.1 Plastic Hinge Model

In order to obtain moderate calculation efforts, a structural modelling with plane bar elements could be adopted, where the elastic or inelastic behavior is carried out through an elastic central zone and two extreme zones with plastic characteristics. Thus, the non-linear material behavior of the bar elements are concentrated on its extremities, since those are the critical zones where cracking occurs, being developed in a short extension, generally not exceeding the cross section height.

For the dynamic analysis of the bridge in the perpendicular direction of the deck axis (transverse direction), a simplified structural model is proposed. Such a model accurately simulates tri-dimensional behavior through a bi-dimensional analysis [13], when the bridge is nearly straight, as is the case. Taking into account that the main behavior of the bridge, for transverse direction actions, is dictated by bending moments on the deck and axial forces and bending moments on the piers, and that there is no significant interaction between torsional

effects on the deck and bending moments on piers, it could be concluded that, for obtaining the bridge response for transverse actions, the coupling between deck and piers could be made only by imposing the same transverse displacement at the points where the deck and the piers are linked. Therefore, with the model illustrated in Figure 1 it is possible to simulate, in a 2-D domain, the links between piers and deck through ties that insure compatibility of displacements, allowing independent rotations. The piers are oriented to have their larger dimension in the plane direction and an axial load equal to the vertical action of the deck must be considered. This plane model is extremely economic in terms of calculation effort, especially when non-linear effects must be considered, but it allows the main aspects of the structural behavior of the bridge for horizontal actions in the transverse direction of the deck axis to be captured in an accurate way. As mentioned above, only the eventual torsion stiffness of the deck mobilized with the rotation of the top extremity of the piers is not included.

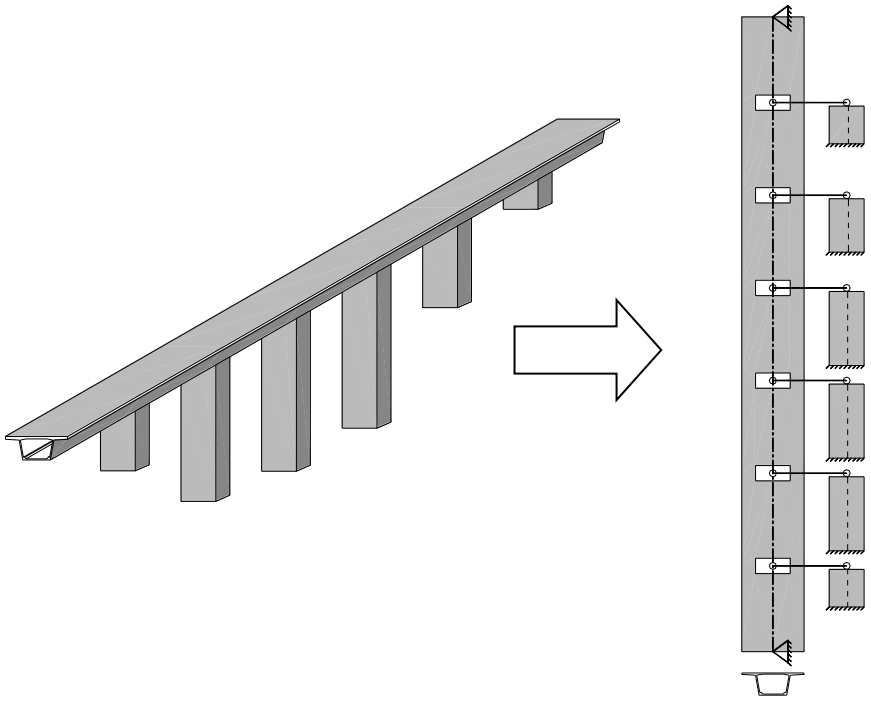

Figure 1: Bridge structural modelling.

To characterize the plastic hinges behavior, a global non-linear model for the sections must be considered. Thus, the moment-curvature loops used in the idealization of the reinforced concrete are obtained by a modified Takeda model [6, 14, 15]. The characterization of these moment-curvature relationships is based on the initial cracking of the concrete and the yielding of the reinforcement that could be obtained from the monotonic material behavior of the reinforced concrete element. Therefore, the laws of monotonic material behavior cloud be numerically established through a procedure based on a cross section fiber model [16], knowing the geometric characteristics of the piers sections, reinforcement dimensions and location, and material characteristics. For the materials behavior several models are available for concrete and steel. An example of possible model that could be adopted for concrete is the

Kent-Park [17], which have in consideration the confined and unconfined properties for monotonic and cyclic behavior. This cross section fiber model also allows the separation of confined and unconfined concrete regions. As for the steel model, the widely used Giuffrè-Menegotto-Pinto model [18] could be adopted, where the Bauschinger effect is considered in the cyclic behavior. The definition of the cyclic stress-strain response can be evaluated through the monotonic stress-strain curve of the structural element, associated with adequate rules that control the response evolution, in load-unload cycles, load inversion and the pinching effect, [6, 15]. The moment-curvature curve (m-ρ), obtained with this procedure, is used to simulate the non-linear behavior and the hysteretic dissipation of energy for the structural seismic response analysis, including the stiffness degradation in the unload case and the pinching effect in the load inversion, essential aspects in the seismic behavior of structures.

2.2 Fiber Model

Fibers models are usually supported by a finite element discretization and based on a modeling section fibers (for concrete and steel fibers), where the non-linear behavior is distributed along the element length and cross-sectional area. Several models have been developed and suggested in the past [2, 3, 16]. Such type of numerical models are carried out with a three-dimensional structural modeling based on finite elements, where the structure is divided into 3D bar elements which are then divided into longitudinal fibers. Therefore, these fibers constitute a mesh at the level of their cross-sections, with no forces interaction between the fibers, i.e. each fiber mobilizes only the force corresponding to the cross section position and material properties. For the distribution of the nonlinearity along the length of the structural elements, a formulation based on its global deformations is performed. The numerical integration of this formulation is carried out at the level of Gauss points of each element. Thus, the behavior of spatial structures subject to static or dynamic loads can be carried out through analyzes that consider the local (beam-column effect) and global (effect of large displacements / rotations) geometric non linearity, as well as the material plasticity.

2.3 Damage Model

This numerical tool is supported on refined finite element (FE) meshes, with high complexity and detail levels in the constitutive laws defined for both concrete and steel. The concrete is simulated with a continuum damage model which is briefly described further on. As for the steel, it could be modelled by applying the well-known and widely used Giuffrè-Menegotto-Pinto model. The continuum damage model used in these applications was initially developed by Faria [4, 19] to characterize the non-linear behavior of large-scale concrete mass structures and has proven to be a powerful tool [20, 21]. Essentially, this model is based on continuum damage mechanics applied to determine a given point stress tensor σ relying on two independent scalar damage variables which account for the non-linearity associated with continuous and irreversible concrete degradation. Such a stress tensor is defined by:

$$\sigma = \left(1 - d^{+}\right)\overline{\sigma}^{+} + \left(1 - d^{-}\right)\overline{\sigma}^{-} \tag{1}$$

where d^{+} and d^{-} are, respectively, the tensile and compressive scalar damage variables, whereas $\overline{\sigma}^{+}$ and $\overline{\sigma}^{-}$ are the corresponding principal tensile and compressive effective stress tensors as defined in Faria and Oliver [19]. The damage variables are controlled by evolution

laws related to material properties r_0^+ and r_0^- (whose initial values are associated with uniaxial tensile and compressive concrete strengths which can be experimentally obtained) and expressed as follows:

$$d^+ = 1 - \frac{r_0^+}{\bar{\tau}^+} \cdot e^{A^+\left(1-\frac{\bar{\tau}^+}{r_0^+}\right)} \quad \text{, for } \bar{\tau}^+ \geq r_0^+ \qquad (2)$$

$$d^- = 1 - \frac{r_0^-}{\bar{\tau}^-} \cdot \left(1 - A^-\right) - A^- \cdot e^{B^-\cdot\left(1-\frac{\bar{\tau}^-}{r_0^-}\right)} \quad \text{, for } \bar{\tau}^- \geq r_0^- \qquad (3)$$

where $\bar{\tau}^+$ and $\bar{\tau}^-$ are equivalent stress quantities derived from the components of tensors $\bar{\sigma}^+$ and $\bar{\sigma}^-$, respectively. The A+, A- and B- parameters must be finely adjusted so that the expected uniaxial tensile and compressive responses can be suitably simulated by the model. The numerical analyses in this work were based on 3D solid FE modelling which, in particular, aimed to realistically simulate the main phenomena associated with shear, with special emphasis on the well-known shear lag effect that is characteristic of I or T shape sections as well as hollow-section elements. Even so, this 3D modelling strategy does not make it possible to directly and totally simulate the confining effects provided by stirrups, particularly concerning the effect of the increased concrete deformation capacity. As such, a complementary strategy was adopted, which consists on conveying these confining effects on the uniaxial compressive curve that is used for defining the A+, A- and B parameters. In this work, both the "confined" and "unconfined" compressive characterization curves are defined according to the proposal by Kent and Park [17], later modified by Park [22]. This strategy is essentially the same as the one used in previous works [20, 21, 23], which was found to yield good results in similar simulation studies.

3 SEISMIC SAFETY ASSESSMENT

Nowadays, several methodologies to assess the seismic safety of structures have being used, since the more complex and general to the more simples and easy to apply. These last ones involve usually more assumptions and simplifications in opposition with the more general methodologies that tries to reproduce the reality as close as possible.

One safety assessment methodology wherein proposed, that correspond to a quite general procedure, can be used for any probability distribution of the seismic action and correspondent vulnerability functions with the desired polynomial approximation (including high order polynomial functions), as well as any probability distribution of the capacity. Although the origins of this methodology go back to the beginning of the 1980s [15, 24, 25], it continues to be developed and used for the calculation of seismic risk for a chosen confidence level. In addition, results obtained by this method may provide an excellent support for calibration of other methods involving simplifying assumptions. The fact that this methodology represents a more general approach for seismic risk assessment may imply a larger number of structural analyses.

In order to evaluate the structural safety with the proposed methodology, it is necessary to calculate the probability of collapse, given by the convolution of the probability distribution of demand with the probability distribution of capacity, [15]. To obtain the demand probability distribution it is necessary to know the probability distribution of the seismic

action and define the so called vulnerability curve, a non-linear function that relates the seismic action with the action effect. Therefore, to establish the vulnerability curve, a seismic response of the bridge for increasing seismic intensities must be computed and, for each intensity level, the maximum response value obtained. This curve relates the seismic magnitude with the maximum value of the parameter chosen for describing the structural response, for example, the maximum ductility demand on the pier base. These values could be adopted as the control parameters for the safety evaluation, bearing in mind that in these structural elements the higher strains and the greater non-linear incursions are developed specially in the zones close to the foundation, which significantly influence the bridge behavior.

Several accelerograms, in order to take into account the stochastic characteristic of earthquakes, should be synthesized, by a random manner, matching the response spectra that characterize the earthquake ground motion. With these accelerograms, the average values of the ductility demanded for each magnitude of seismic action are obtained and polynomial functions can be adjusted through this series of points, thus obtaining the vulnerability functions of each pier, and, consequently, of the bridge, illustrated with the curve number 3 in Figure 2. The intensity of an earthquake could be defined by the peak acceleration value in the horizontal direction, a. To a given region, these intensities should be estimated by combining i) seismological information expressed by: generation models, distribution of location, magnitude and intensity of a past earthquake in the region and ii) geological and geotechnical data [24]. The maximum annual values of peak acceleration can be computed using generation models based on the magnitude values and source locations observed from past earthquakes; magnitudes being transformed into bedrock accelerations by means of attenuation formula. The characteristic value of the distribution of peak acceleration, a_k, to 50 years of the structure life time, is equal to the 0.95 fractile (975 years of return period) of the annual extreme distribution, a_{975}, as stated by Eq(4).

$$F(a_k) = \left(1 - \frac{1}{975}\right)^{50} = 0.95 \tag{4}$$

The most important part of the distribution of maximum peak accelerations in 975 years can be identified as an extreme type I probability distribution [26, 27]. Thus, the seismic action, represented as curve number 1 in Figure 2, can be characterized by the following equation, Eq (5):

$$f(a) = \alpha . \exp\left(y - \exp(y)\right) \tag{5}$$

with $y = -\alpha(a - u)$ and where α and u are the parameters that characterize the extreme distribution. The information that allows the estimation of the variation coefficient of the probability distribution of maximum peak acceleration in 975 years is scarce. The value of 0.5 can be adopted, taking in consideration the research made by Borges and Castanheta [24], to the Portuguese territory. In this case, considering the characteristic value of the peak acceleration predicted to Lisbon, a_k = 219,4cm/s^2, that corresponds to a medium seismicity zone, the parameters of the extreme distribution α = 22,5E-3 and u = 87.4cm/s^2 are obtained.

A transformation of this action through the vulnerability function is carried out, and the action effect in the bridge obtained, more precisely in each of its piers, once the vulnerability function for each pier can be defined through the bridge response (curve 3 in Figure 2). Thus the probability density function of the action effect, f_{EA}, expressed in demanded ductilities is

obtained (curve 4 in Figure 2) and the corresponding probability distribution of maximum ductility demand, F_{EA}, is achieved.

For the capacity characterisation of pier sections - in this case their available ductility - a probability density function, f_R , was considered (curve 2 in Figure 2). This function could be defined through the mean ductility, μ_d, and its variation coefficient, VC, by means of a simulation method, the Latin Hypercubic Sampling, as employed by Delgado *et al.* [28].

Finally, the collapse probability of the bridge is evaluated through the integration of the convolution function, Eq (6) and curve number 5 in Figure 2, defined through the probability distribution function of the action effect, F_{EA} - expressed in maximum ductilities demanded in the bridge - and the capacity probability density function, f_R - expressed in available ductilities, [24, 25].

$$C(\mu) = (1 - F_{EA}) \cdot f_R \tag{6}$$

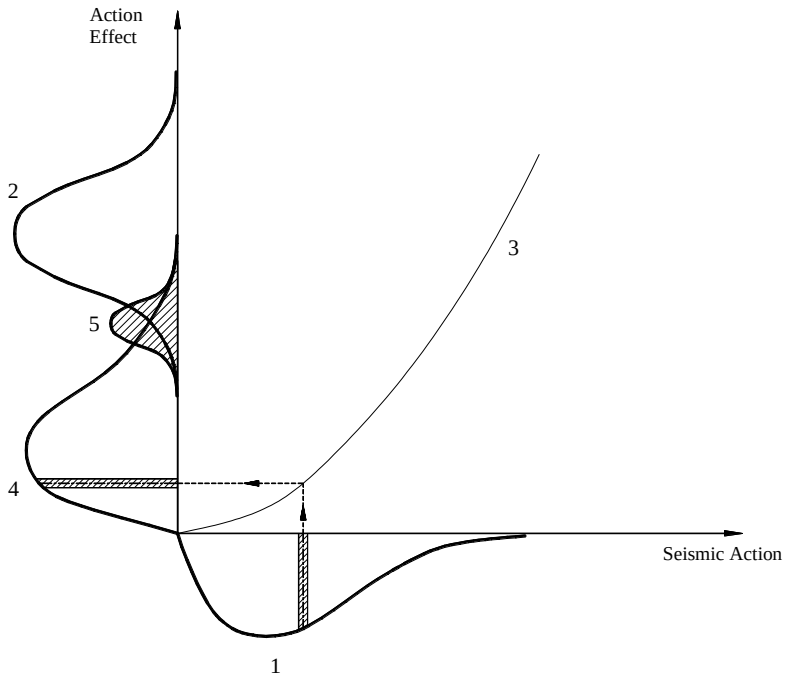

Figure 2: Graphic representation of safety assessment procedure.

4 APPLICATION TO THE TALÜBERGANG WARTH'S BRIDGE

The first application, corresponds to the Talübergang Warth's bridge, built in the seventies in Vienna and designed for a low seismic level, where the comparison and calibration of the numerical simulations were carried out. For this purpose, static analysis were performed to the bridge piers with imposed displacements on the pier top end. This bridge was the main study purpose on the scope of a European project, Vulnerability Assessment of Motorway Bridges (VAB). The reinforced concrete Talübergang Warth bridge is located approximately 63 km to south of Vienna and it is constituted by a continuous deck, with five central spans of 67m and two extreme spans of 62m, supported by piers with rectangular hollow section, pinned in their connection to the deck and fully-fixed in the base, where is concentrated the largest seismic effects. This bridge is constituted by six piers with heights between 16.9 and 38.9 meters and identical rectangular hollow sections in concrete, being the external dimensions of 2.5x6.8m2

with the largest dimension in the transverse direction of the deck axis, and with a walls thickness of 0.3m along the largest dimension of the section of the pier and 0.5m along the smallest. In Figure 3 the geometry of the bridge is illustrated, with the further on adopted designation for the piers, and in Table 1 the piers height are presented, measured from the top of the foundation to the deck base.

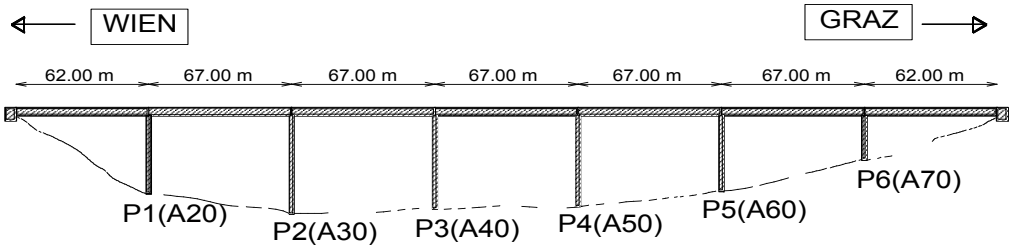

Deck section properties:

Area : 10.02062 m^2
Prin. moment of inertia Y : 124.3786 m^4
Prin. moment of inertia Z : 34.77017 m^4
Torsional constant : 52.84362 m^4

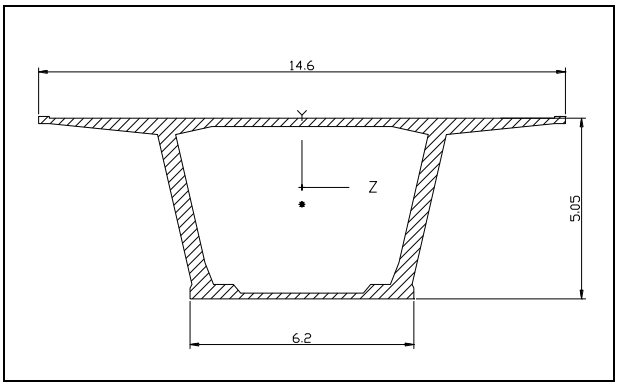

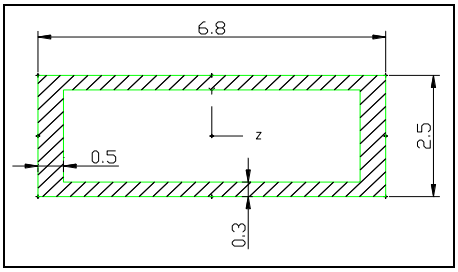

Pier section properties:

Area : 5.98 m^2
Prin. moment of inertia Y : 34.61394 m^4
Prin. moment of inertia Z : 5.538984 m^4
Shear ratio Y : 3.40178
Shear ratio Z : 1.736134
Torsional constant : 15.12595 m^4

Figure 3: Warth Bridge Geometry.

Pier	P1 (A20)	P2 (A30)	P3 (A40)	P4 (A50)	P5 (A60)	P6 (A70)
L (m)	29.8	38.9	37.8	36.0	30.0	16.9

Table 1: Piers height.

4.1 Non-linear material behavior of the piers sections

All the piers have the same transverse hollow section in concrete, with the external dimensions of 2.5x6.8m^2 and the interiors, corresponding to the hollow interior zone, of 1.9x5.8m^2. The piers longitudinal reinforcement is suppressed along its height in three regions, but it is distributed evenly in the transverse section. For all the piers the transverse reinforcement spacing is 20 cm, constituted by a single rectangular stirrup in each of the four walls of the hollow section, with an 8 mm diameter rebar for the current section and a 12 mm diameter rebar in a zone of 1m close to the basis of each pier. For all the piers, a 4cm thick cover concrete was used.

The concrete of the piers bridge is the B400, with a maximum compression tension of 43.0 MPa and a Young modulus of 33.5 GPa. The concrete confinement depends on the efficiency of the stirrups. In this case, very small values are adopted, due to the much reduced confinement obtained with the transverse reinforcement, since only the four corners of the piers are really confined. The steel is the type TR50 according to the supplied design project, and a bilinear curve was adopted, defined through a Young modulus of 200 GPa and a yielding tension of 545.0 MPa, being considered that no hardening exists, therefore with a horizontal yielding.

The axial force resulting from the deck and the piers weights are the following: 26460kN for the pier P1, 28633kN for the pier P2, 28473kN for the pier P3, 28218kN for the pier P4, 27353kN for the pier P5 and 24610kN for the pier P6.

In Figure 4 the moment-curvature curves computed at the base of piers P3 and P6 are illustrated, with several structural models.

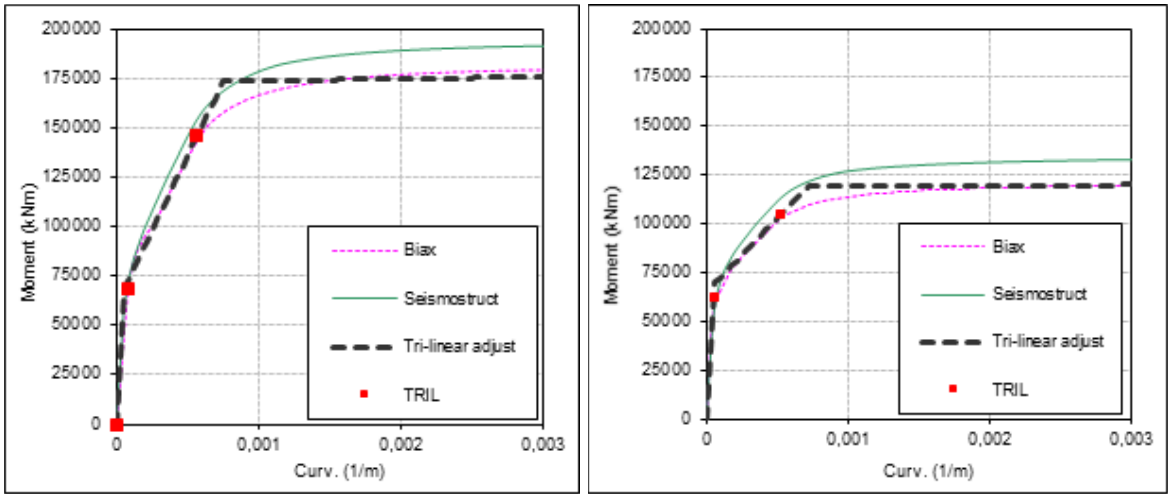

Figure 4: Moment-curvature curves at the base of piers P3 (left) e P6 (right).

Using the cross section fiber model, Biax [16, 29] the moment-curvature curves with dot line were obtained, computing the section moment for a given curvature and axial force applied to the pier. Based on this curves, tri-linear laws were adjusted for the monotonic loading, ruling the piers non-linear behavior in the plastic hinge model (the PNL program). For this application the fiber model adopted was the Seismostruct program, where the moment-curvature monotonic curve (solid line) at the piers base was obtained through a pushover analysis. The concrete first crack and the steel first yielding in the cross section at the piers base were also computed with the analytical equations programmed (TRIL), developed by Arêde [30] and illustrated (in Figure 4) with square points.

As it can be seen, the curves obtained with the cross section fiber model (Biax) and with the fiber model (Seismostruct) are reasonably close, but the ultimate moment value is higher in the Seismostruct program. For the plastic hinges model (PNL), these monotonic laws are the basis for the characterization of the piers cyclic behavior, involving alterations to their initial characteristics, caused by the cyclic loads, simulating the strength and stiffness degradation, as well as the pinching effect.

4.2 Pier response to imposed top displacements

The analysis of the piers for cyclic loads is presented, corresponding to a horizontal displacement law applied to their top extremities, and considering an independent operation in each of them. The displacement is applied in the free extremity of the pier (P3 e P6) and in the largest transverse direction, therefore, in the perpendicular direction of the deck axis. The displacement time history imposed on the piers, corresponds to the application of twelve semi-cycles with 4 levels of growing intensity. For pier P3, the intensity levels correspond to 0.08m, 0.18m, 0.35m and 0.62 and, for pier P6, the intensity levels correspond to 0.02m, 0.07m, 0.14m and 0.25.

These experimental cyclic tests were carried out at Ispra laboratory, Italy, giving a good basis for comparing the results obtained by the different numerical models. It was also possible to compare the results with a damage model carried out by Vila Pouca [20], as referred before one much more refined (and accurate) methodology based on finite elements. Figure 5 illustrated the force-displacement relationships obtained experimentally and numerically (PNL, Seismostruct and Damage Model) on the top of the piers, due to the displacement time history imposed on the piers. The force values and the dissipated energy of these numerical results are very close to the experimental results of Ispra [31, 32], showing the good performance of the numerical model used for simulating the inelastic behavior of the piers under cyclic loads.

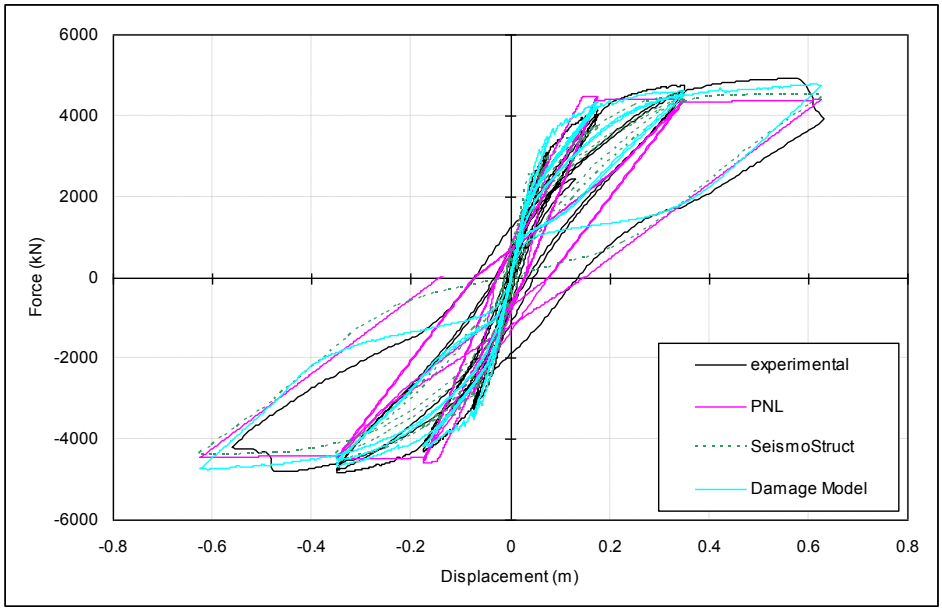

a) Pier P3

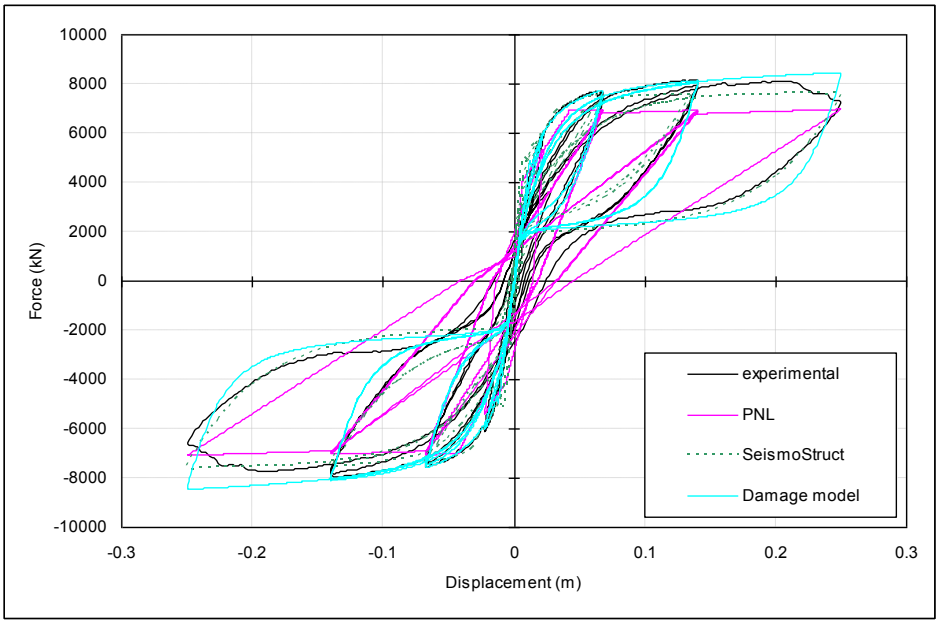

b) Pier P6

Figure 5: Force-displacement curves.

5 APPLICATION TO THE PREC8 BRIDGE

This second application, corresponds to one reinforced concrete bridge experimentally studied at the Joint Research Centre, in Ispra, in the scope of the PREC8 (Prenormative Research in support of EuroCode 8), on which several studies are known. The methodologies for numerical simulation of bridges were applied in order to study its possibilities and the ability to assess the seismic behavior of reinforced concrete structures. In addition, the bridge seismic risk assessment, involving a larger number of structural analyses, was also performed.

This bridge is a reinforced concrete bridge experimentally studied at the Joint Research Centre, in Ispra, in the scope of the PREC8 (Prenormative Research in support of EuroCode 8), subjected to experimental and numerical studies, which constitutes an excellent basis for the calibration of the proposed models for the seismic safety assessment of bridges.

Many methods of analysis were used to this bridge but as it is stated in the report n.º 4, November 1996, ECOEST/PREC8 (G.M Calvi and P. E. Pinto) there is an acute need of analytical tools for non-linear dynamics analysis which are simple and economical to use and provide answers of acceptable levels of accuracy. Therefore, this application is an effort to contribute for the development of analytical tools.

The experimental studies [2] were accomplished on a reduced scale model of this bridge, represented in Figure 6, whose geometric characteristics correspond to a deck with four spans of 20m each and three piers of hollow section, 5.6, 2.8 and 8.4m in height, fully-fixed in the base and pinned in their connection to the deck.

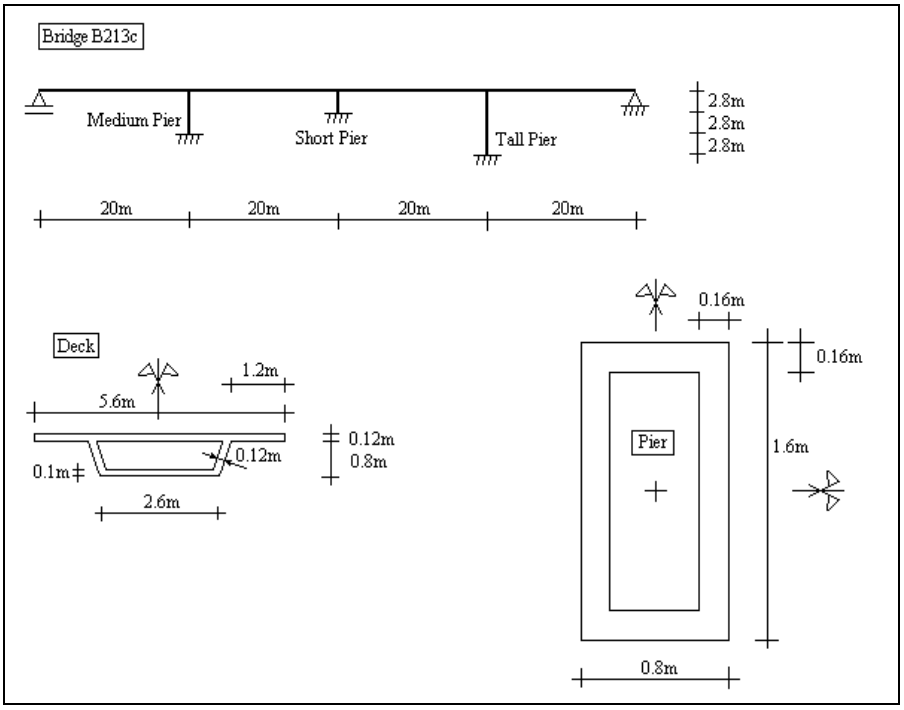

Figure 6: Scaled bridge geometry.

5.1 Non-linear material behavior of the piers sections

The bridge was designed for a peak ground acceleration of 0.35g (343cm/s^2) in medium soil condition (soil type B) and applying the EC8 provisions. The longitudinal reinforcement of the tall and medium piers is 7680mm^2 (1.15%) and of the short pier, 3330mm^2 (0.5%), being the current spacing of the transverse reinforcement of 80mm. In the first 1.5m next to the pier base, the confinement is better, once the spacing between stirrups is smaller, being 60mm to the tall and medium piers and 50mm to the short pier. In the model the same reinforcement cover of 8mm was used for all the piers. Figure 7 illustrates the localization and the section diameters of the longitudinal reinforcement, as well as the transverse reinforcement details, with close stirrups assembling steel bars alternatively.

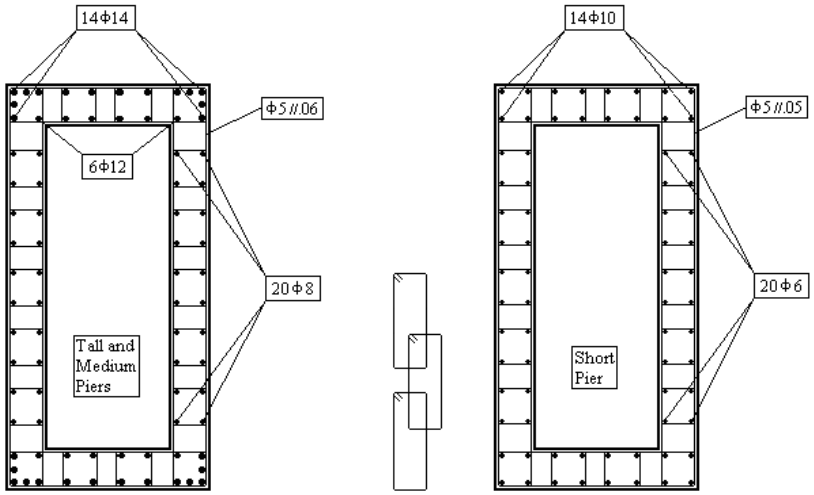

Figure 7: Piers reinforcement.

In agreement with the supplied project details, the bridge piers concrete presents a maximum stress compression of 39.0 MPa and a Young modulus of 25 GPa. The confinement depends on the efficiency of the stirrups in the concrete jacketing, adopting for this case a confinement coefficient corresponding to a transverse reinforcement rate of ρ_v = 0.00555 [33].

For the steel a bilinear curve was adopted, defined through a Young modulus of 206 GPa and a yielding tension of 500.0 MPa, considering that no hardening exists, therefore with a horizontal yielding.

The moment-curvature curves were obtained by using the abovementioned cross section fiber model and, for a given curvature and the axial strain of the piers, the corresponding moment was evaluated. The axial strain in the piers was considered equal to 1700kN. Based on these curves, tri-linear laws were adjusted for a monotonic loading that simulates the non-linear behavior of the piers. These laws are the basis for the cyclic behavior definition of the piers, involving alterations to their initial characteristics, caused by the cyclic loads, simulating the strength and stiffness degradation, as well as the pinching effect [6].

5.2 Pier response to imposed top displacements

The analysis of the piers for cyclic loads is presented, corresponding to a horizontal displacement law applied to their top extremities, and considering an independent operation in each of them. The displacement application was accomplished in the free extremity of the pier and in the largest transverse direction, therefore, in the perpendicular direction of the deck axis.

In order to simulate the isolated behavior of each pier, the structural modelling was carried out only considering a vertical bar, composed by a central zone with linear and elastic behavior, and two zones in the bar extremities with inelastic behavior - the plastic hinges, where the non-linear behavior of the pier is concentrated. It was considered 0.8m for the length of the plastic hinge (*lp*), about half of the cross section height of the pier [33].

The displacement time history imposed on the piers top corresponds to the application of twelve semi-cycles of growing intensity.

Figure 8 represents the force-displacement relationships obtained numerically on the top of the tall and short piers, due to the displacement time history imposed on the piers. The force values and the dissipated energy of these numerical results are very close to the experimental results of Ispra [2], showing the good performance of the numerical model used for simulating the inelastic behavior of the piers under cyclic loads.

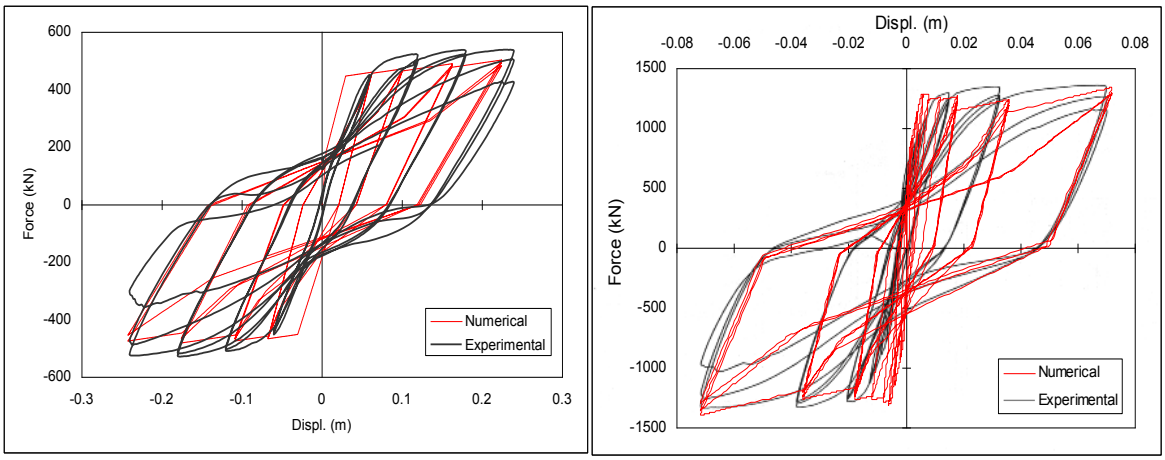

Figure 8: Force-displacement curves for the tall pier (left) and short pier (right).

5.3 Seismic response

For the dynamic and non-linear analysis of the bridge several accelerograms should be used to take into account the stochastic characteristic of earthquakes, but in this application only the generated artificial accelerogram compatible with the response spectrum of the EC8, and used in Ispra [2], was considered. The numerical analysis was performed on the reduced scale model of the bridge (Figure 6), with a scale factor of 2.5, and so the peak acceleration and duration of the accelerogram were, respectively, multiplied and divided by this factor, obtaining 0.875g and 4s.

The discretization of the structure was made with 22 elements, the deck comprising 16 elements and the connecting ties and piers six elements. The deck bars and the connecting ties have elastic linear behavior, while the piers are made up of bars with plastic hinges, 0.8m long, at their extremities. Hence, the non-linear behavior of the structure is concentrated on the piers, more precisely at their plastic hinges close to the foundation, an acceptable assumption, since those will be the zones of the structure with greater strength during seismic action.

Due to the hysteretic material behavior when subjected to cyclic loadings, the hinges carry the main responsibility for energy dissipation in the structure, so a null structural damping was considered, only bearing in mind the hysteretic mechanism with regard to energy dissipation.

Figure 9 illustrates the comparison of the medium, short and tall piers top displacement response obtained numerically with the plastic hinge model (black curve) with the ones obtained in Ispra, by Guedes [2], which corresponds to the numerical analyses with a fiber model (grey curve with the label: Numerical MG) and the experimental results (black dashed curve).

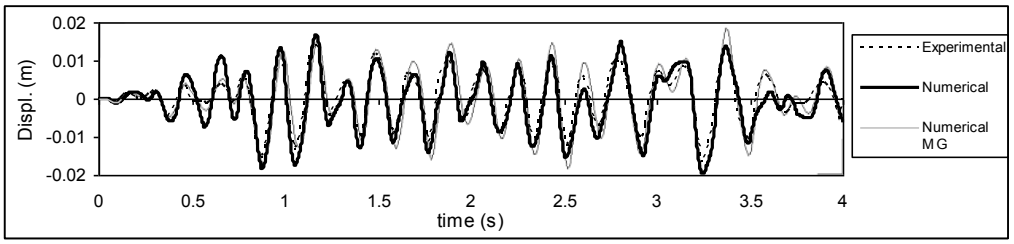

a) Medium pier

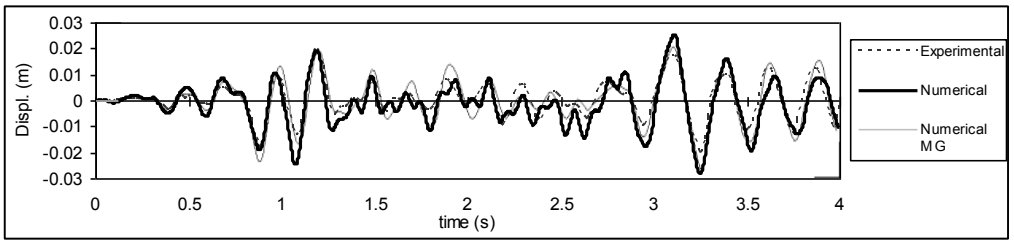

b) Short pier

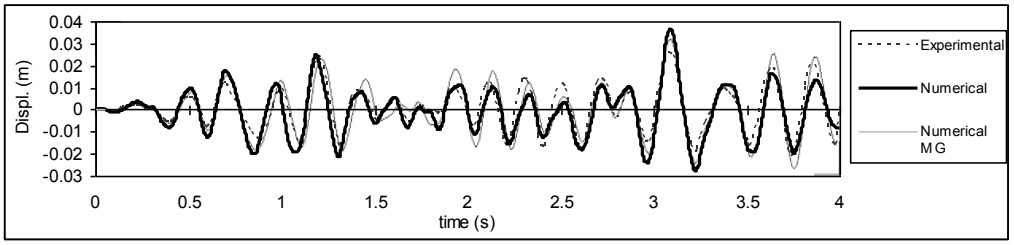

c) Tall pier

Figure 9: Seismic response of the piers.

The seismic response obtained for the three piers is reasonably close with the experimental results, as much in frequency as in maximum values, thus demonstrating a satisfactory behavior. As it could also be seen, the solution obtained with the plastic hinge numerical approach has, in general, values a little bit lower than the experimental ones meanwhile the solution obtained by Guedes (referred as Numerical MG) has values a little bit greater. This illustrates the sensibility of the numerical non-linear dynamic analysis to the material parameters used when comparative analysis with experimental tests is made. In this application the problem is even greater because the boundary conditions could cause lower displacements in the numerical analysis, once in laboratory testing it is not possible to completely restrict the displacements at the piers base, especially the base rotation, as it was done in the present analysis where zero displacements were prescribed.

Furthermore, during the experimental campaign a local deformation on the foundation connection with the pier was observed (Report EUR 16358 by Guedes and Pinto [34]). The numerical analysis carried out by Guedes has considered an additional elastic element between the pier and the foundation (with a support hinge at top of this element) to simulate the rotational deformation (without horizontal displacement) and accurately reproduce the experimental tests. The same strategy was performed in the plastic hinge model, using elastic characteristics for the additional elements in a way that the elastic stiffness of the piers become similar to the experimental conditions. The length of these additional elements was

0.025m and the Young modulus was: 0.13 GPa for medium pier, 0.04 GPa for short pier and 0.10 GPa for tall pier.

As expected, the short pier has the more significant non-linear behavior and, conversely, the tall one has the lesser non-linear behavior, being the closest to the experimental result.

5.4 Safety assessment

In the Portuguese code, to obtain the design value of the peak acceleration the characteristic value must be multiplied by a safety factor of 1.5, therefore the design earthquake and the extreme probability distribution of the action are referred to the same acceleration, about 0.35g, once the safety analysis was carried out in the full scale bridge (prototype).

In order to obtain the vulnerability curves of the piers, different intensities of the referred earthquake were increasingly applied to the bridge. Therefore, from each peak acceleration value the corresponding moment-curvature result was obtained, allowing the evaluation of the maximum ductility demanded at the piers base, the values adopted as the control parameters to evaluate the safety assessment of the piers.

Using the least-squares method, polynomial functions of 2nd order were adjusted through a series of points of the demanded ductilities for each level of seismic action, obtaining relationships between action and action effects that characterize the vulnerability functions of each pier, as represented in Figure 10.

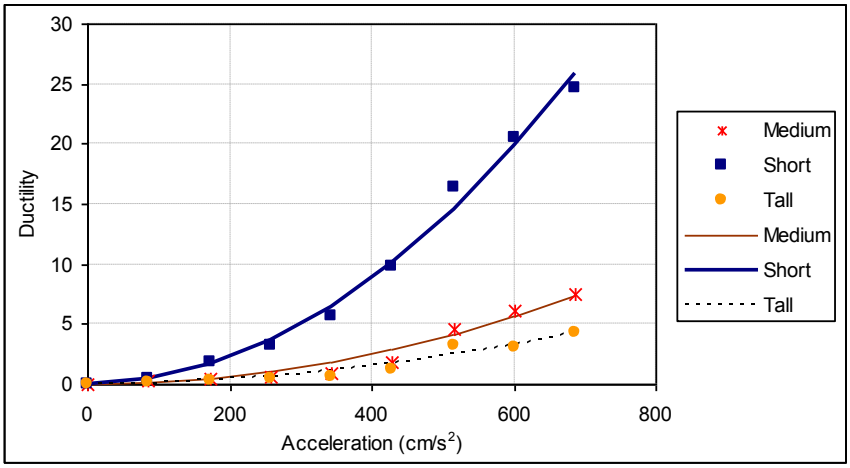

Figure 10: Vulnerability functions of the piers.

To quantify the collapse probability of the bridge, a sensitive analysis was carried out with different values for the characterization of the piers strength function - referred before in Figure 2 as curve number 2. In Table 2 the collapse probability values for each pier are referred to, given that the strength density function is defined by a normal distribution function with mean ductility values of 4, 8 and 12, and variation coefficient values of 0.05 and 0.20.

Pier	VC = 0.05			VC = 0.20		
	$\mu_{d=4}$	$\mu_{d=8}$	$\mu_{d=12}$	$\mu_{d=4}$	$\mu_{d=8}$	$\mu_{d=12}$
Short	0.0002689	0.0000462	0.0000093	0.0060939	0.0015345	0.0004698
Medium	0.0000003	0.0000000	0.0000000	0.0000213	0.0000023	0.0000016
Tall	0.0000000	0.0000000	0.0000000	0.0000011	0.0000005	0.0000006

Table 2: Collapse Probabilities.

As expected, observing at Table 2, the greater collapse probabilities occur consistently in the short pier (which correspond the more severe vulnerability functions), for any pair of mean ductility and variation coefficient values, being the one that controls the safety of the bridge. It is also possible to verify that the collapse probability increase for lower values of mean ductility and greater values of variation coefficient. The safety evaluation therefore shows that only for large available ductility and low variation coefficients values the bridge presents a collapse probability close to a reasonable limit ($\approx 10^{-5}$).

These values of collapse probability were computed considering that a flexural failure mechanism has occurred before the shear strength reaches the capacity value and, therefore, no brittle failure in shear was achieved in any pier. The experimental tests at Ispra have showed that the collapse mechanism was achieved with a horizontal crack at the base of the short pier, with the failure of the reinforcement bar in tension. To prove that, the shear capacity in the plastic hinges of the piers was computed, using the equations of Priestley *et al.* [35] and assuming high ductility: Medium pier – 1185kN; Short pier – 1375kN and Tall pier – 1115kN. These values were not achieved in the piers base (plastic hinge) when the plastic moment capacity was reached.

6 CONCLUSIONS

In this work several numerical models were suggested for the cyclic and seismic responses of RC bridges, involving different approaches for the consideration of the structural modeling (plane or tri-dimensional behavior of the bridge) and for the simulation of the non-linear behavior. One methodology for seismic safety assessment of bridges, involving the evaluation of its failure probability, was also presented.

Two applications were carried out with the proposed methodologies, which shows good accuracy for the structural assessment analyses of bridges subjected to cyclic and seismic loading confirmed by the excellent comparison of the obtained results with experimental responses. For calibration of the methodologies, the first application was mainly focus on the bridge piers static and cyclic analysis, of which several experimental and numerical results are known, allowing the comparison of results and evidencing the potentiality of the numerical models. The comparison of different approaches for the monotonic response of the cross section moment-curvature was performed, with quite good comparison of results. For cyclic response of the piers, with imposed top displacements, several numerical model simulations were carried out, allowing to conclude that all responses were satisfactorily close to the experimental tests.

An irregular bridge was used for seismic analysis, with numerical simulations performed with plastic hinge model and fiber model. The numerical responses obtained compares quite well with the experimental results, both in the maximum displacement values and the frequencies. This models also allows the seismic response of the bridge to be obtained in a

realistic way, with reduced calculation efforts and a reasonable simplicity, which is a necessary condition for studies of risk assessment where a great number of analyses are required. Taking pier ductility as the control parameter, the seismic vulnerability of the bridge was evaluated, for different values of mean ductilities and variation coefficient of the strength distribution function. The safety evaluation performed provided the conclusion that the bridge only presents a collapse probability below an acceptable level for μd = 12 and VC = 0.05, demonstrating the total inability of this irregular bridge in dealing with earthquake loadings.

REFERENCES

[1] Taucer, F., Spacone, E., & Filippou, F.C. A Fiber Beam-Column Element for Seismic Response Analysis of R/C Structures, *Report EERC 91-17, Earthquake Engineering Research Center*. University of California. Berkeley, 1991.

[2] Guedes, J. Seismic Behaviour of Reinforced Concrete Bridges – Modelling, Numerical Analysis and Experimental Assessment. *PhD Thesis*, FEUP, Porto, 1997.

[3] SeismoSoft. SeismoStruct - A computer program for static and dynamic nonlinear analysis of framed structures [online], 2004. Available from URL: http://www.seismosoft.com.

[4] Faria, R., Oliver, J. and Cervera, M. A strain based plastic viscous damage model for massive concrete structures, *International Journal of Solids and Structures* 35(14), 1533-1558, 1998.

[5] Vecchio, F.J., & Collins, M.P. Predicting the response of reinforced concrete beams subjected to shear using modified compression field theory. *ACI structural journal* – technical paper, 258-268, American Concrete Institute, 1988.

[6] Costa & Costa hysteretic model. RC Frames Under Earthquake Loading. *CEB; Comité Euro-International du Béton*, Bulletin nº231, 1996.

[7] Arêde, A. Seismic Assessment of Reinforced Concrete Frame Structures with a New Flexibility Based Element, *PhD Thesis*, FEUP, Porto, 1997.

[8] Kang, H.D., Willam K., Shing, B. and Spacone E. Failure analysis of R/C columns using a triaxial concrete model, *Computers and Structures* 77, 423-440, 2000.

[9] Liu, J. and Foster S.J. A three-dimensional finite element model for confined concrete structures, *Computers and Structures* 77, 441-451, 2000.

[10] Kwon, M. and Spacone E. Three-dimensional finite element analyses of reinforced concrete columns, *Computers and Structures* 80, 199-212, 2002.

[11] Papanikolaou, V.K. and Kappos A.J. Numerical study of confinement effectiveness in solid and hollow reinforced concrete bridge piers: Methodology, *Computers and Structures* 87, 1427-1439, 2009.

[12] Papanikolaou, V.K. and Kappos A.J. Numerical study of confinement effectiveness in solid and hollow reinforced concrete bridge piers: Analysis results and discussion, *Computers and Structures* 87, 1440-1450, 2009.

[13] Delgado, P., Costa, A., & Delgado, R. A Simple Methodology for Seismic Safety Assessment of Bridges. *12ECEE - The Twelfth European Conference on Earthquake Engineering*, London, UK, 9-13 September, 2002.

[14] Takeda, T., Sozen, M.A., & Nielsen, N.N. Reinforced concrete response to simulated earthquakes. *Journal of the Structural Mechanics Division of the ASCE*, ST12, 96, 1970.

[15] Duarte, R.T., Oliveira, C.S., Costa, A.C., & Costa, A.G. A Non-linear Model for Seismic Analysis, Design and Safety Assessment of Reinforced Concrete Buildings. *Earthquake Damage Evaluation & Vulnerability Analysis of Building Structures*, edited by A.Koridze, OMEGA Scientific, 1990.

[16] Vaz, C. T. Comportamento Sísmico de Pontes com Pilares de Betão Armado, *PhD Thesis*, FEUP/LNEC, 1992. (in Portuguese)

[17] Kent, D. & Park, R. Flexural Members with Confined Concrete, *Journal of Structural Division* 97(7), 1969-1990, ASCE, 1971.

[18] Menegotto, M., & Pinto, P.E. Method of Analysis for Cyclically Loaded R.C. Plane Frames Including Changes in Geometry and Non-Elastic Behavior of Elements Under Combined Normal Force and Bending. *Symposium on Resistance and Ultimate Deformability of Structures Acted On by Well Defined Repeated Loads*, IABS Reports Vol. 13, Lisbon, 1973.

[19] Faria, R. and Oliver, J. A rate dependent plastic-damage constitutive model for large scale computations in concrete structures, *CIMNE Monograph* 17, Barcelona, 1993.

[20] Vila Pouca, N. Simulação Numérica da Resposta Sísmica de Elementos Laminares em Betão Armado, *PhD Thesis*, FEUP, Porto, 2001 (in Portuguese).

[21] Faria, R., Vila Pouca, N. and Delgado, R. Simulation of the cyclic behaviour of R/C rectangular hollow section bridge piers via a detailed numerical model, *Journal of Earthquake Engineering* 8(5), 725-748, 2004 (DOI:10.1142/S1363246904001547).

[22] Park, R., Priestley, M. and Gill, W. Ductility of Square-Confined Concrete Columns, *Journal of Structural Division* 108(4), 929-950, ASCE, 1982.

[23] Faria, R., Vila Pouca, N. and Delgado, R. Seismic behaviour of an R/C wall: Numerical simulation and experimental validation, *Journal of Earthquake Engineering* 6(4), 473-498, 2002.

[24] Borges, J. F., & Castanheta, M. *Structural Safety*; Curso 101, 3ª Edition, LNEC, Lisbon, 1982.

[25] Costa, A. G. Seismic Analysis of Irregular Structures. *PhD Thesis*, FEUP, Porto, 1989. (in Portuguese)

[26] Oliveira, C. S., Sousa, M. L., & Costa, A. C. Definition of Seismic Action in the Context of EC-8. Topics for Discussion, *12th World Conference on Earthquake Engineering*, Auckland, New Zealand, 1999.

[27] Costa, A. C. A Acção dos Sismos e o Comportamento das Estruturas. *PhD Thesis*, FEUP, Porto, 1993. (in Portuguese)

[28] Delgado, J. M., Azeredo, M., & Delgado R. M. Probability of failure estimation of current reinforced structures using the Latin Hypercube Sampling. *RISK ANALYSIS II*, pp. 105-114, Editor C.A. Brebbia, Wit Press, Southampton, Boston, 2000.

[29] Varum, H. Modelos Numéricos para a Análise Sísmica de Pórticos Planos de Betão Armado, *MSc Thesis*, FEUP, Porto, 1996. (in Portuguese)

[30] Arêde, A. Seismic Assessment of Reinforced Concrete Frame Structures with a New Flexibility Based Element, *PhD Thesis*, FEUP, Porto, 1997.

[31] Pinto, A.; Pegon P.; Magonette G.; Molina J.; Buchet P.;Tsionis G. Pseudodynamic Tests on a Large-Scale Model of na Existing RC Bridge Using Non-linear Substructuring and Asynchronous Motion, *EUR 20525 EN, Joint Research Centre*, Ispra, Italy, 2002.

[32] Gago, A.; Varum, H.; Pinto, A.V. Preliminary Non-linear Analyses of a Reinforced Concrete Bridge, *VAB Project, Joint Research Centre*, Ispra, 1999.

[33] Delgado, P. (2009). Avaliação da Segurança Sísmica de Pontes. *Ph.D. thesis*, FEUP (in Portuguese), (http://ncrep.fe.up.pt/web/artigos/PDelgado_PhD_Thesis.pdf).

[34] Guedes, J., & Pinto, A. V. Numerical Simulation of the ELSA PSD Tests of R/C Bridges, *Report EUR 16358 EN*, EC, JRC, Ispra, Italy, 1996.

[35] Priestley, M.J.N., Seible, F., & Calvi, G.M. *Seismic Design and Retrofit of Bridges*. New York, 1996.